scientific reports

Check for updates

OPEN

Accurate quantification of cell-free *Ceruloplasmin* mRNA as a biomarker for early detection of hepatocellular carcinoma

Minh Ngo[1,2], Trang Dao[3], Trang Hoang[3], Ung Nguyen[3], Jakob Stenman[4], Huy Duong[1] & Tho Ho[3,5]✉

Accurate and early detection of hepatocellular carcinoma (HCC) is critical for improving patient outcomes. Current biomarkers like AFP have limited sensitivity, necessitating novel diagnostic markers. A novel semi-nested RT-PCR assay was developed to quantify circulating *Ceruloplasmin* (*CP*) mRNA in peripheral blood. This method co-amplifies *CP* mRNA and an internal control (IC) gene, followed by DNA melting analysis to distinguish and quantify *CP* mRNA. *CP* mRNA levels were significantly higher in the HCC group (median: 3.37) compared to both the CLD group (0.24, $p = 0.0066$) and the HD group (0.17, $p < 0.0001$). Further analysis using ROC curves highlighted the diagnostic performance of the assay. For differentiating HCC from CLD, the area under the ROC curve (AUC) was 0.704, with 50.98% sensitivity and 95.24% specificity. In comparison to HD, the AUC was 0.812, with 74.51% sensitivity and 80.65% specificity. Against the combined control group (CLD and HD), the AUC was 0.768, with 50.98% sensitivity and 96.15% specificity. Additionally, in 59.1% of HCC cases with AFP levels below 20 ng/mL, *CP* mRNA levels were elevated, indicating that *CP* mRNA could help detect a substantial proportion of AFP-negative HCC cases. This study, the first comprehensive clinical investigation of cell-free *CP* mRNA for HCC diagnosis, demonstrates its potential as a sensitive and specific non-invasive biomarker. Further validation in larger cohorts is needed to confirm its clinical utility.

Keywords Hepatocellular carcinoma (HCC), Circulating *CP* mRNA, Semi-nested RT-PCR, Biomarker, DNA melting analysis, Liquid biopsy

Hepatocellular carcinoma (HCC) is the sixth most common cancer and third leading cause of cancer-related deaths globally[1]. Early detection is crucial for effective treatment, yet current diagnostic methods are limited, leading to poor prognosis[2]. Diagnosis typically involves imaging techniques like ultrasound (US), CT scans, MRI, and blood tests for AFP and PIVKA II[3,4]. However, these methods generally lack cost-effectiveness and accuracy for large at-risk groups. Abdominal US, while non-invasive and relatively inexpensive, depends heavily on the skill of the physician performing the ultrasound, making it challenging to deploy on a large scale. Adding a specific HCC biomarker could improve screening accuracy[5].

In this context, liquid biopsy—analyzing blood-based biomarkers such as circulating tumor cells (CTCs), circulating tumor DNA (ctDNA), and exosomes—emerges as a promising non-invasive alternative[6]. While traditional biomarkers like CTCs and ctDNA are well-studied, cell-free RNA (cfRNA) in plasma represents a new and promising area in cancer research[7]. cfRNAs are released into the blood plasma through mechanisms such as passive leakage from necrotic or apoptotic cells, as well as active secretion via extracellular vesicles like exosomes. However, cfRNA is inherently unstable and susceptible to degradation unless protected by extracellular vesicles, exosomes, or nucleoproteins, which allow for its transport in the bloodstream[8]. Recent advances in cancer diagnostics have demonstrated that profiling cfRNA in plasma can effectively differentiate

[1]Department of Gastroenterology and Hepatology, 103 Military Hospital, Vietnam Military Medical University, Hanoi, Vietnam. [2]Radiology Center, 103 Military Hospital, Vietnam Military Medical University, Hanoi, Vietnam. [3]Department of Genomics and Cytogenetics, Institute of Biomedicine and Pharmacy (IBP), Vietnam Military Medical University, Hanoi, Vietnam. [4]Childhood Cancer Research Unit, Department of Women's and Children's Health, Karolinska Institutet, Stockholm, Sweden. [5]Department of Microbiology, 103 Military Hospital, Vietnam Military Medical University, Hanoi, Vietnam. ✉email: hohuutho@vmmu.edu.vn

cancer patients from non-cancer individuals and those with precancerous conditions[9]. For HCC, specific gene sets, including *ceruloplasmin* (*CP*) mRNA, have shown promise by revealing a gradual transition in expression levels from non-cancerous states through cirrhosis to HCC. Although this method has demonstrated high accuracy in distinguishing HCC from cirrhosis and non-cancer groups, the required deep sequencing and complex bioinformatics pose challenges for widespread, routine use, particularly in resource-limited settings.

Furthermore, the technical challenge in detecting *CP* mRNA lies not only in its very low concentration in peripheral blood but also in accurately measuring the subtle variations of *CP* mRNA levels among patients with HCC[8,10]. These minute variations are critical for early diagnosis and monitoring disease progression, necessitating a detection method with exceptional sensitivity and precision. Therefore, establishing a quantitative PCR-based method for accurately quantifying cell-free *CP* mRNA is necessary to make this promising diagnostic approach more accessible and practical for widespread clinical use.

To address these challenges, a novel and rapid assay has been developed to accurately quantify *CP* mRNA from a plasma sample. This study aims to develop and validate a novel quantitative approach for measuring cell-free *CP* mRNA levels in the peripheral blood of patients with primary HCC. Leveraging the sensitivity and specificity of semi-nested reverse transcription polymerase chain reaction (rt-PCR) combined with DNA melting analysis, we propose a method that not only allows for the accurate quantification of *CP* mRNA but also incorporates an internal control (IC) for normalization and quality control. This dual strategy enhances the assay's ability to detect slight changes in *CP* mRNA concentration, thus providing a reliable and sensitive tool for early cancer detection and monitoring.

Through this approach, the study seeks to explore the clinical significance of minute fluctuations in *CP* mRNA levels measured in HCC patients, highlighting the potential of *CP* mRNA as a biomarker. The innovative assay presented in this research represents a significant advancement in the field of liquid biopsy, offering a non-invasive, highly sensitive method for the early detection of HCC, tracking disease progression, and informing therapeutic decisions, thereby contributing to improved patient outcomes.

Materials and methods

Subjects and methods

Over the period from July 2021 to April 2024, participants were enrolled from the 103 Military Hospital. The aim was to gather blood plasma samples from 103 individuals to thoroughly evaluate the new quantitative PCR assay for detecting circulating *CP* mRNA. The cohort included 51 HCC patients and 52 control participants, which comprised both 31 healthy donors and 21 individuals with chronic liver conditions like cirrhosis and hepatitis.

HCC was diagnosed in accordance with the guidelines set by the American Association for the Study of Liver Diseases (AASLD 2018)[11], with liver biopsies used to confirm any cases that were inconclusive. The stage of HCC was classified according to the Barcelona Clinic Liver Cancer (BCLC) staging system, 2022 update. In this study, small hepatocellular carcinoma (HCC) lesions were detected during routine surveillance of patients with chronic liver disease. Surveillance included ultrasound and alpha-fetoprotein (AFP) measurement every six months. Lesions ≥ 1 cm identified on ultrasound, AFP levels ≥ 20 ng/mL, or a doubling of AFP values prompted further investigation with contrast-enhanced computed tomography (CT) or magnetic resonance imaging (MRI). Lesions were classified using the Liver Imaging Reporting and Data System (LI-RADS). Histopathological confirmation was performed for lesions with inconclusive imaging results or atypical findings.

Participants with chronic hepatitis B were diagnosed according to the EASL 2017 Clinical Practice Guidelines on the management of hepatitis B virus infection. The diagnostic criteria involved the detection of HBsAg in the serum for more than six months, alongside elevated serum HBV DNA levels and liver function tests indicating chronic liver inflammation. Liver cirrhosis was also diagnosed based on the EASL 2017 guidelines, using clinical signs (jaundice, ascites, hepatic encephalopathy), laboratory tests (serum albumin, bilirubin, prothrombin time), and imaging techniques (ultrasound, transient elastography, liver biopsy). Control participants were verified to be free of liver cancer through comprehensive physical examinations.

All participants were fully briefed on the study's goals and nature, and they provided informed consent to participate. This process of obtaining informed consent ensured a solid foundation for the analysis, thereby enhancing the validity and reliability of the study's findings. The experimental protocol was approved by the Institutional Review Board of the 103 Military Hospital, Vietnam Military Medical University (reference number: 12/2021/CNChT-HĐĐĐ, dated 28/06/2021).

Sample collection and processing

Blood Collection: Approximately 10 mL of venous blood was collected from each participant into K2 EDTA tubes to prevent clotting. The blood samples were processed within six hours to separate the plasma, which was subsequently stored at − 80 °C.

RNA Extraction and Quality Assessment: RNA from the plasma was extracted using the QIAamp Circulating Nucleic Acid Kit (Qiagen, Germany). The extracted RNA's quantity and quality were measured with a Nanodrop spectrophotometer to ensure they were suitable for further analysis.

Total RNA was isolated using a QIamp circulating Nucleic acid Kit (Qiagen, Germany) from plasma samples according to the manufacturer's instructions. The extracted RNA samples were then stored at − 80 °C until used.

Quantification of *CP* mRNA

The semi-nested RT-PCR method was utilized to amplify and quantify the circulating mRNA of the *CP* gene in plasma samples. RT-PCR simultaneously amplifies *CP* mRNA and an in-vitro synthesized RNA of a non-human IC gene (Table 1). In the first round of amplification, primers CP-Fo and CP-Ro were used for the *CP* gene, and IC-Fo and IC-Ro for the internal control RNA, which is an artificially synthesized sequence unrelated to human genes (Table 1).

Amplification round	Primers/probe	Sequence (5′-3′)
1st PCR round	Forward primer (CP-Fo)	CGACGTAAAACGACGGCCAGT-CCATCTGAAAGCCGGTTTGC
	Reverse primer (CP-Ro)	CTGGCATATCATGACATACGACCTGA-ACATGCTTCCCACGG
	Forward primer (IC-Fo)	CGACGTAAAACGACGGCCAGT-ACTAGCGTGCCTTTGTAA
	Reverse primer (IC-Ro)	CTGGCATATCATGACATACGACCTGA-GAGCGATACGAGCA
2nd PCR round	Forward primer (CP-Fi)	CCAGGTCCAGGAGTGTAA
	Forward primer (IC-Fi)	CTCATTCGTTTCGGAAGAGC
	Reverse primer (U-Ri)	CTGGCATATCATGACATACGACCTGA
Internal control's sequence (IC)		CGGCGTAATACGACTCACTATAGGGATGAACCGACGACGACTAC AGCGTGCCTTTGTAAGCACAAGCTGATGAGTACGAACTTATGTAC TCATTCGTTTCGGAAGAGCGGGCGGCTGCTCGCGGATACCCGTAC CTCGGGTTTCCGTCTTGCTCGTATCGCTCGAGAACGCAAGTTCTGT TAACGTGAGTCTTGTAAAACCTTCTTTTTACGTTTACTCTCGTGTTA AAAATCTGAATTCTTCTAGAGTTCCTGATCTTC

Table 1. Primer, probe, and internal control (IC) sequences. Note: The underlined regions indicate synthetic non-human sequences added to the 5′ ends.

The forward and reverse primers have non-complementary, non-human sequences attached to their 5' ends, with the 5′ end of the reverse primers for both target genes (CP-Ro, IC-Ro) sharing an identical sequence, serving as the binding site for the reverse primer in the second round of amplification. Each primer was used at a concentration of 0.2 µM. The final concentration of the master mix was 1 × HTOne Ultra RT-qPCR Probe master mix (HT Biotec, Vietnam). The template RNA extracted from plasma was used at a volume of 2.5 µl per reaction, and 7.5×10^3 copies of IC RNA were added to each RT-PCR reaction.

The first round of amplification was performed using the Applied Biosystems 9800 FAST Thermal Cycler (Thermo Fisher Scientific, USA) with the following thermal cycling conditions: reverse transcription at 25 °C for 2 min, followed by 55 °C for 10 min, succeeded by denaturation at 95 °C for 2 min. The amplification process included an initial cycle of denaturation at 95 °C for 15 s, annealing at 63 °C for 30 s, and extension at 72 °C for 30 s. This was followed by 18 cycles of denaturation at 94 °C for 15 s, annealing at 76 °C for 30 s, and extension at 72 °C for 30 s. The reaction was then held at 4 °C indefinitely.

In the second round of PCR amplification, a common reverse primer (U-Ri) is used for both target genes. The entire sequence of the U-Ri primer is identical to the 5′ sequence of the reverse primers used in the first round, which includes a non-complementary region at the 5′ end that does not pair with the target gene sequences. The forward primers (CP-Fi for the *CP* gene and IC-Fi for the internal control) are specific to their respective target genes and bind within the sequence amplified in the first round (Table 1). Each primer is used at a concentration of 0.2 µM, and the master mix is 1 × HTOne MaX qPCR Green master mix (HT Biotec, Vietnam). The amplification is performed using the Rotor-Gene Q instrument (Qiagen, Germany) with the following thermal cycling conditions: an initial denaturation at 95 °C for 15 min, followed by 35 cycles of 94 °C for 15 s, 63 °C for 30 s, and 72 °C for 30 s. After the standard amplification cycles, a DNA melting curve analysis is performed to determine the melting temperature peaks of the PCR products. The target gene (*CP* mRNA) shows a melting temperature (Tm) of about 79.1 °C, and the IC has a Tm of about 86.1 °C. Samples containing the target mRNA yield two distinct melting peaks corresponding to the CP and IC PCR products. The concentration of the *CP* mRNA is determined by comparing the melting peak ratios of the target gene to the IC, enabling accurate quantification of *CP* mRNA levels in the sample.

To evaluate the precision of our semi-nested RT-PCR assay, we measured *CP* mRNA levels from the same plasma sample across five independent runs. RNA was extracted from the same plasma sample for each run, and the coefficient of variation (CV) was calculated to assess the consistency of the assay across these runs. The CV provides an estimate of the reproducibility of the assay when applied repeatedly to the same sample.

To further validate the sensitivity of the assay, a head-to-head comparison with a qRT-PCR assay using TaqMan probe was performed. The semi-nested RT-PCR demonstrated a 20-fold higher analytical sensitivity (see Supplementary Data for detailed methodology and data).

Data analysis

For the analysis, we utilized the melting profile, F(T), between 70 and 90 °C, which was exported from the raw data of the Rotor-Gene Q instrument (Qiagen, Germany). Each spectrum was normalized to a range of [0,1] by simple min–max scaling, which standardized melting spectra from varying settings or experiment batches. After normalizing the data of the function F(T), we calculated the values of the function − dF(T)/dT and averaged three neighboring points. The peak heights were determined based on these values using Microsoft Excel.

To determine the peak height of the DNA melting curves related to the *CP* mRNA and IC RNA, the height of each peak is calculated by subtracting the height of the peak's baseline from the peak's maximum height. The

baseline height for the *CP* peak is averaged over the temperature range of 75–76 °C, while the baseline for the IC peak is averaged over the range of 88–89 °C (Fig. 1).

Data were analyzed using MedCalc software version 20.019 (MedCalc Software Ltd, Ostend, Belgium). Quantitative data were presented as median (interquartile range) and percentages. Proportions between groups were compared using Student's t-test, while differences in group medians were analyzed using the Mann–Whitney test. Receiver Operating Characteristic (ROC) curve analysis was employed to establish cutoff points that optimize sensitivity, specificity, and diagnostic accuracy. The diagnostic performance was evaluated using the area under the ROC curve (AUC), sensitivity, specificity, and Youden index. Odds ratios were calculated to determine the association between *CP* mRNA levels and HCC.

Results and discussion

Study population characteristics

The study included 103 participants divided into three main groups (Table 2): 51 patients with hepatocellular carcinoma (HCC), 21 patients with chronic liver disease (CLD) and 31 healthy donors (HD). The median age in the HCC group was 62 years, significantly higher than both the CLD group and HD group ($p < 0.05$). Gender distribution was predominantly male, with 96.1% males in the HCC group, 95.2% in the CLD group and 90.3% in the HD group.

Liver function tests and tumor marker levels were evaluated. The HCC group exhibited significantly higher levels of ALT and AST compared to the control group ($p < 0.05$), indicating more severe liver dysfunction. The presence of cirrhosis and risk factors such as HBV and HCV infections were prevalent in the HCC group, with 43.1% having cirrhosis and 82.4% having HBV infection.

These detailed demographic and clinical characteristics provided a comprehensive foundation for evaluating the diagnostic performance of the *CP* mRNA assay.

Overview of RT-PCR assay for *CP* mRNA quantification

A novel quantitative RT-PCR assay was developed to accurately quantify circulating *CP* mRNA in peripheral blood. This assay features two rounds of amplification (semi-nested), enhancing sensitivity and specificity. The first round involves simultaneous amplification of *CP* mRNA and an in-vitro synthesized RNA of a non-human internal control (IC) gene. The primers used include CP-Fo and CP-Ro for the *CP* gene, and IC-Fo and IC-Ro

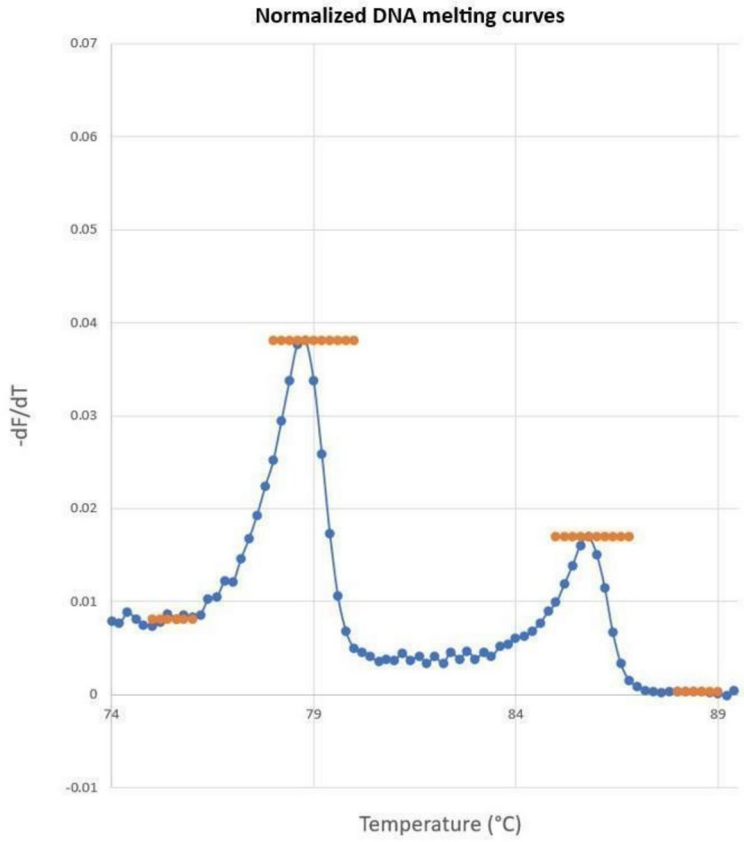

Fig. 1. Normalized melting curves and peak height determination for *CP* mRNA and IC RNA. Peak heights were determined by subtracting the baseline height from the peak's maximum height. The baseline for the CP peak was averaged over 75–76 °C, while the baseline for the IC peak was averaged over 88–89 °C. The ratio of these peak heights reflects the concentration of *CP* relative to IC.

Characteristic	Category	HCC group[a] (n = 51)	CLD[b] (n = 21)	HD[c] (n = 31)	*p* value
Gender	Male n (%)	49 (96.1%)	20 (95.2%)	28 (90.3%)	> 0.05
	Female n (%)	2 (3.9%)	1 (4.8%)	3 (9.7%)	
Age (years)	< 50	10 (19.6%)	15 (71.4%)	16 (51.6%)	**< 0.05**
	50–59	12 (23.5%)	1 (4.8%)	7 (22.6%)	
	60–69	16 (31.4%)	5 (23.8%)	4 (12.9%)	
	> 70	13 (25.5%)	0 (0%)	4 (12.9%)	
	Median (IQR)	62 (50.3–69.8)	45 (41.0–55. 3)	49.0 (37.3–60.5)	p(a,b) = 0.00* p(a,c) = 0.01*
PLT	Median (IQR)	163.0 (115.0–192.0)	173.0 (127.0–210. 5)	–	–
Prothrombin %	Median (IQR)	82 (75.3–88.8)	–	–	–
INR	Median (IQR)	1.15 (1.08–1.22)	–	–	–
Albumin	Median (IQR)	38.0 (36.0–40.85)	–	–	–
Bilirubin total	Median (IQR)	15.5 (11.96–20.98)	13.5 (10.7–17.5)	–	–
PIVKA II (n = 17)	Median (IQR)	580.0 (86.01–4328.04)	–	–	–
AFP	Median (IQR)	35.13 (9.47–1426.92)	3.44 (2.35–4.34)	–	–
AST	Median (IQR)	49.76 (35.3–98.5)	29.7 (26.0–53.9)	25.96 (22.9–31.0)	**$P_{a,c} < 0.05$ $P_{b,c} < 0.05$**
ALT	Median (IQR)	43.44 (33.0–62.7)	36.53 (25.2–47.1)	22.49 (17.5–25.5)	**$P_{a,c} < 0.05$ $P_{b,c} < 0.05$**
Cirrhosis	Yes	22 (43.1%)	6 (28.6%)	0 (0%)	–
	No	29 (56.9%)	15 (71.4%)	31 (100%)	–
Risk factor	HBV	42 (82.4%)	21 (100.0%)	0	–
	HCV	7 (13.7%)	0 (0%)	0	–
	Alcohol-related	11 (21.6%)	–	0	–
Number of tumors	Single n (%)	28 (54.9%)			–
	Two n (%)	11 (21.6%)			–
	Three n (%)	1 (2.0%)			–
	More than Three n (%)	11 (21.6%)			–
Greatest diameter (mm)	Median (IQR)	42 (28.2–74.5)			–
Tumor location	Right lobe n (%)	27 (52.9%)			–
	Left lobe n (%)	9 (17.7%)			–
	Both n (%)	15 (29.4%)			–
Vascular invasion	Yes	12 (23.5%)			–
	No	39 (76.5%)			–
Metastatic Lymph Node	Yes	3 (5.9%)			–
	No	48 (94.1%)			–
Extrahepatic spread	Yes	6 (11.8%)			–
	No	45 (88.2%)			–
BCLC stage	0,A	28 (54.9%)		–	–
	B	8 (15.7%)		–	–
	C	13 (25.5%)		–	–
	D	2 (3.9%)		–	–

Table 2. Demographic, laboratory tests and tumor-related characteristics of study groups. Significant values are in [bold].

for the internal control RNA (Fig. 2, panel i). Both the forward and reverse primers for each gene contain a non-complementary sequence at the 5′ end (Table 1, underlined regions) to ensure effective annealing at a high temperature of 76 °C. This selective annealing temperature ensures amplification of cDNA synthesized from *CP* mRNA while preventing genomic DNA amplification, which can only bind to the primers at the short 3′ regions.

The reverse primers for both target genes contain a non-complementary sequence at the 5′ end, which serves as the binding site for the common reverse primer (U-Ri) in the second round. These reverse primers also function as gene-specific reverse transcription primers, as their 3′ ends have sequences that specifically bind to the target genes, facilitating cDNA synthesis from RNA (Fig. 2, panel ii).

In the second round of PCR, a common reverse primer (U-Ri) is used for both target genes (Fig. 2, panel iv). This ensures that the *CP* and IC genes are amplified with comparable efficiency, facilitating accurate determination of the ratio of *CP* mRNA to the internal control. The forward primers (CP-Fi for CP and IC-Fi for IC) are specific to their respective target genes (Fig. 2, panel iii). The amplification products are then subjected to DNA melting curve analysis to determine the melting temperature peaks, with the target gene (*CP* mRNA)

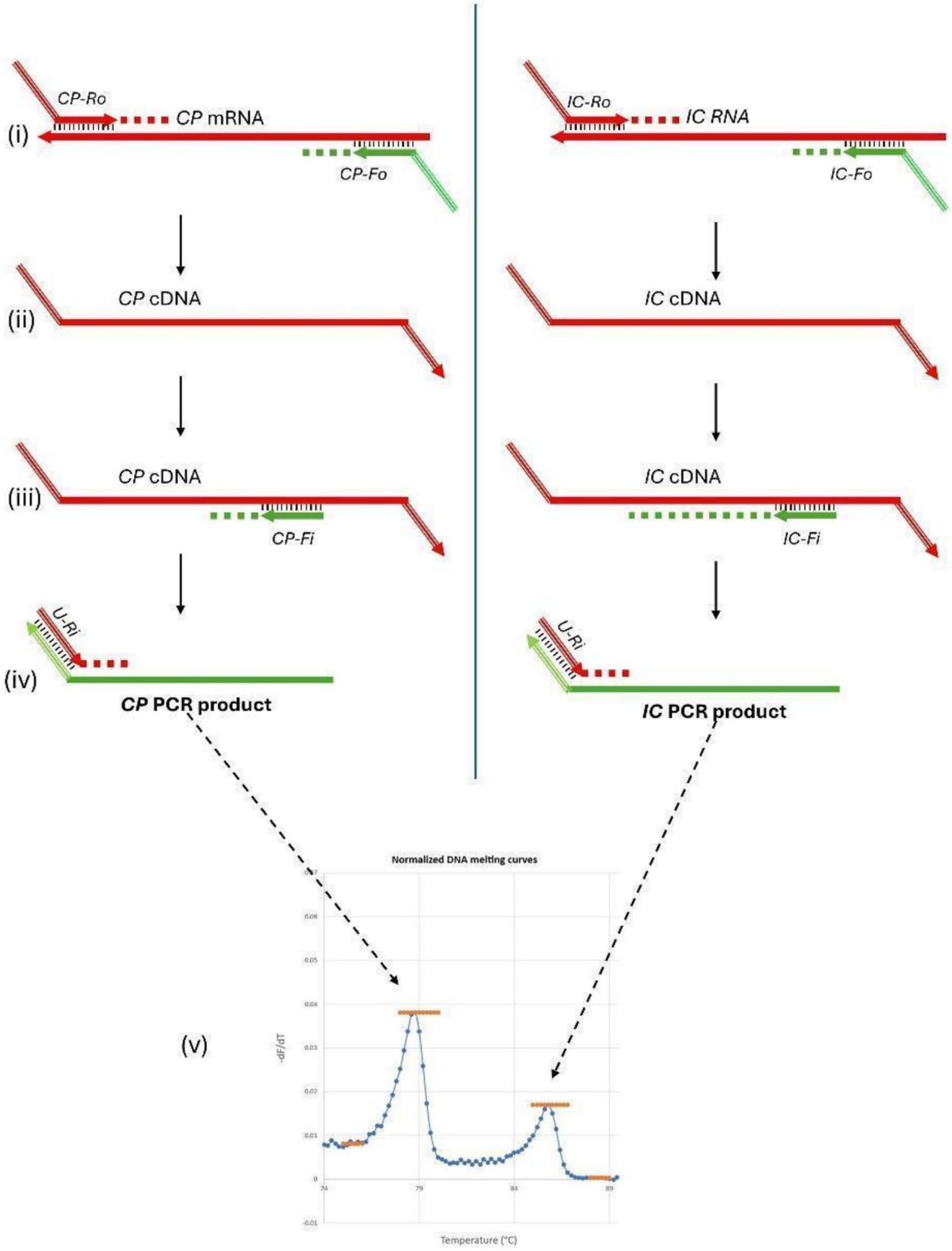

Fig. 2. Schematics of the semi-nested RT-PCR assay for *CP* mRNA quantification. The novel quantitative RT-PCR assay for *CP* mRNA involves two rounds of amplification to enhance sensitivity and specificity. The first round uses specific primers for CP and an internal control (IC) gene, incorporating non-complementary sequences at the 5' ends (Fig. 2, panel i). These primers also function in reverse transcription to synthesize cDNA (Fig. 2, panel ii). The second round employs a common reverse primer (U-Ri) for both genes (Fig. 2, panel iv) and specific forward primers (CP-Fi and IC-Fi) (Fig. 2, panel iii). The amplified products are analyzed via DNA melting curve to distinguish *CP* mRNA and IC peaks (Fig. 2, panel v). The relative concentration of *CP* mRNA is quantified by calculating the ratio of the CP peak height to the IC peak height.

showing a melting temperature (Tm) of approximately 79.1 °C and the IC showing a Tm of approximately 86.1 °C (Fig. 2, panel v). This analysis allows for the identification of two distinct melting peaks corresponding to the CP and IC PCR products.

In this method, the ratio of the peak heights reflects the concentration of CP relative to the fixed concentration of IC. Therefore, small changes in *CP* concentration can alter this ratio, enabling the detection of subtle variations in *CP* mRNA levels in peripheral blood samples. The consistent amplification efficiency ensured by the common reverse primer and the use of a fixed concentration of IC allows for the detection of small changes in *CP* mRNA levels, which are critical for early diagnosis and monitoring of disease progression. The optimal amount of IC RNA added to the reactions was determined experimentally through exploratory tests on a small group of HCC and non-cancer samples to provide the best differentiation between HCC and control groups.

Diagnostics performance of circulating *CP* mRNA for HCC

The precision of the semi-nested RT-PCR assay was evaluated through five independent runs, with RNA extracted from the same plasma sample each time. The coefficient of variation (CV), calculated from the CP/IC ratio across these runs, was 28.21%, indicating acceptable reproducibility and precision for this assay. Although there was some variability in the repeated measurements, the overall consistency is considered suitable for ongoing studies and potential clinical applications. To address pre-analytical reliability, *CP* mRNA levels were also assessed in plasma from six patients at three time points: 0, 3, and 6 h after blood collection. No significant variation was observed (Friedman test, $p = 0.311$), and visual inspection of log-scale plots confirmed the temporal stability of *CP* mRNA levels within each patient, despite inter-individual variability, supporting the robustness of the assay under routine pre-analytical conditions.

Building on this acceptable level of precision, the novel quantitative RT-PCR assay demonstrated significant diagnostic effectiveness in distinguishing HCC from non-HCC conditions, including chronic liver disease and healthy controls. The median *CP* mRNA levels, as shown in Fig. 3 (box plot), were significantly higher in the HCC group (3.37) compared to both the chronic liver disease group (0.24, $p = 0.0066$) and the healthy controls (0.17, $p < 0.0001$). This clear difference highlights the potential utility of *CP* mRNA as a biomarker for distinguishing HCC from non-cancerous conditions.

The observed differences in *CP* mRNA levels are further supported by emerging evidence on the stability of cfRNA in plasma, which bolsters its suitability for diagnostic applications. Recent studies have demonstrated that cfRNA, including cf-mRNA, is encapsulated within extracellular vesicles (EVs). These EVs act as protective carriers, shielding cfRNA from degradation in RNase-rich plasma environments[12]. While the present study did not directly evaluate *CP* mRNA stability over time, the robust structural protection provided by EVs suggests that *CP* mRNA can maintain its integrity during routine sample handling. This inherent stability further validates *CP* mRNA as a reliable biomarker for HCC detection and enhances confidence in the observed diagnostic differences.

Further analysis using ROC curves, as shown in Fig. 4, highlighted the assay's diagnostic strength across various comparisons. In differentiating HCC from chronic liver disease, the area under the curve (AUC) was 0.704, with a sensitivity of 50.98% and specificity of 95.24%, using a cutoff of > 3.24 (Youden index = 0.4622). The odds ratio for this differentiation was 20.8 (95% CI 2.593 to 166.835, $p = 0.0043$). When distinguishing HCC

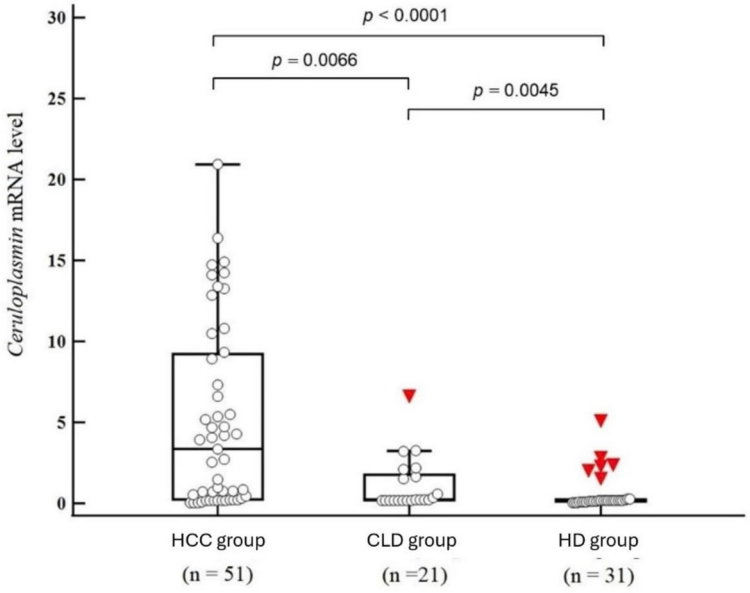

Fig. 3. Comparison of *CP* mRNA levels between HCC and control groups (chronic liver disease and healthy controls). The box plots depict the median and interquartile ranges of *CP* mRNA levels in each group, showing significantly higher levels in the HCC group compared to both the chronic liver disease group ($p = 0.0066$) and the healthy control group ($p < 0.0001$).

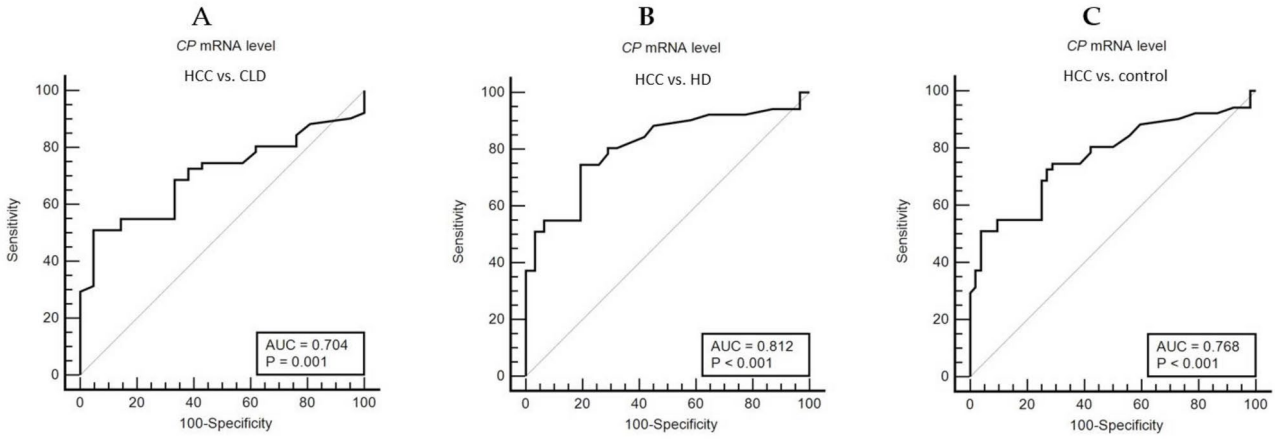

Fig. 4. ROC curve analysis for cell-free *CP* mRNA level in distinguishing HCC from non-HCC conditions. The ROC curves illustrate the diagnostic performance of *CP* mRNA in three comparisons: (**A**) HCC vs. chronic liver disease (AUC = 0.704, sensitivity = 50.98%, specificity = 95.24%, cutoff = 3.24); (**B**) HCC vs. healthy controls (AUC = 0.812, sensitivity = 74.51%, specificity = 80.65%, cutoff = 0.28), and (**C**) HCC vs. the combined control group (AUC = 0.768, sensitivity = 50.98%, specificity = 96.15%, cutoff = 3.24).

from healthy controls, the AUC was 0.812, with a sensitivity of 74.51% and specificity of 80.65%, using a cutoff of > 0.28 (Youden index = 0.5515), and the odds ratio was 12.18 (95% CI 4.090 to 36.266, $p < 0.0001$). Finally, when assessing HCC relative to the combined control group (both chronic liver disease and healthy controls), the AUC was 0.768, with a sensitivity of 50.98% and specificity of 96.15%, using a cutoff of > 3.24 (Youden index = 0.4713), and an odds ratio of 26.00 (95% CI 5.708 to 118.434, $p < 0.0001$).

These findings highlight the assay's good specificity and ability to discriminate HCC from non-HCC conditions, particularly in differentiating HCC from chronic liver disease, reinforcing *CP* mRNA as a valuable biomarker for early detection and diagnosis of HCC.

The method also showed promise in detecting early-stage HCC (BCLC 0 and A) from the combined control group (chronic liver disease and healthy donors), with an AUC of 0.721, (95% CI 0.610 to 0.816) and *p*-value of 0.0006 (Fig. 5). In terms of *CP* mRNA concentrations across different stages of HCC, the median *CP* mRNA levels were 1.105 (0.2–5.43) for early and very early stages (BCLC 0 and A, n = 28), 1.71 (0.25–13.76) for intermediate-stage (BCLC B, n = 8), and 5.17 (1.592–12.638) for advanced stages (BCLC C and D, n = 15). While the comparison between early and very early stages with intermediate stages showed no statistically significant difference ($p = 0.7753$), the trend towards higher *CP* mRNA levels in advanced stages, compared to early and very early stages, approached significance ($p = 0.0543$). It is important to note that the small sample size in the intermediate and late-stage groups may have contributed to the lack of statistical significance. These findings suggest that higher *CP* mRNA levels might be associated with disease progression, and the assay has potential as a sensitive and non-invasive tool for early detection and monitoring of HCC, which is crucial for improving patient outcomes and supporting personalized treatment strategies.

The diagnostic performance of *CP* mRNA and AFP was evaluated using ROC curve analysis. For distinguishing HCC from chronic liver disease, *CP* mRNA (cut-off: 0.28) achieved an AUC of 0.704 (95% CI 0.579–0.829), with a sensitivity of 74.51% and a specificity of 57.1%. In comparison, AFP (cut-off: 20 ng/mL) demonstrated a markedly higher AUC of 0.908 (95% CI 0.833–0.983), with a sensitivity of 56.86% and a specificity of 95.24%. Although AFP exhibited a superior AUC and specificity, CP mRNA showed better sensitivity, which is particularly important for detecting cases in early HCC stages. Among the 22 patients with AFP levels below 20 ng/mL, 13 patients (59.1%) had *CP* mRNA levels above 0.28, indicating that *CP* mRNA could help detect a substantial proportion of HCC cases with low AFP levels (Table 3). Fisher's exact test demonstrated a statistically significant association between *CP* mRNA and AFP levels ($p = 0.0497$). This result highlights the potential of *CP* mRNA as a complementary biomarker to AFP, especially in cases where AFP is not elevated. By identifying cases that AFP might miss, *CP* mRNA offers additional diagnostic value and could play a pivotal role in enhancing early detection efforts for HCC.

In the early and very early HCC stages (BCLC 0 and A, n = 28), *CP* mRNA demonstrated promising performance, with 19 patients (67.9%) having CP mRNA levels above the cut-off of 0.28. In contrast, only 13 of these patients (46.4%) had AFP levels ≥ 20 ng/mL. Furthermore, among the 15 very early and early-stage patients with AFP levels below 20 ng/mL, *CP* mRNA detected 8 cases (53.3%), underscoring its capability to identify cases that AFP might miss.

These findings suggest that *CP* mRNA complements AFP by bridging diagnostic gaps in cases where AFP levels are below the diagnostic threshold, particularly in early-stage HCC. While AFP's higher AUC highlights its superior overall diagnostic performance, *CP* mRNA provides additional diagnostic value by improving detection in challenging scenarios, such as AFP-negative or early-stage HCC. Together, these biomarkers offer a synergistic approach to enhancing the diagnostic accuracy and management of HCC.

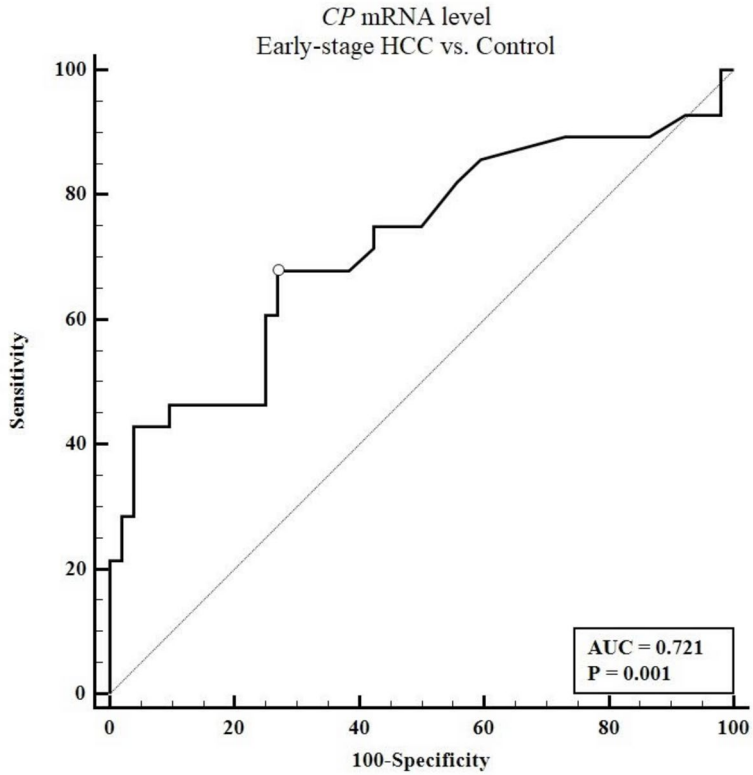

Fig. 5. ROC curve analysis for cell-free *CP* mRNA level in distinguishing early and very early-stage HCC from the combined control group.

AFP level (ng/mL)	*CP* mRNA (> = 0.28)	*CP* mRNA (< 0.28)	Total
AFP < 20	13	9	22
AFP > = 20	25	4	29
Total	38	13	51

Table 3. Association between *CP* mRNA levels and AFP status in HCC patients.

We acknowledge the significant contribution of Roskams-Hieter et al.[9] who demonstrated the diagnostic potential of *CP* mRNA using qRT-PCR to distinguish HCC from non-cancerous conditions. However, a direct comparison with their method is limited by the lack of key methodological details in their publication, such as primer sequences, thermal cycling conditions, and normalization strategies for cfRNA quantification. Building on their work, our study advances the field by introducing a semi-nested RT-PCR assay optimized for quantifying circulating *CP* mRNA, featuring enhanced sensitivity and specificity via two rounds of amplification and robust internal controls. With detailed methodological transparency, our study complements the insights of Roskams-Hieter et al. while providing a foundation for future collaborative validation in larger, prospective cohorts, including a focus on early HCC detection.

HCC is a common malignant disease driven by various underlying pathological pathways, making it challenging to characterize solely with one biomarker. Currently, biomarkers like AFP and PIVKA II are utilized predominantly in clinical practice for primary HCC diagnosis[13,14]. However, their sensitivity often falls short[15]. Therefore, there is a need for novel blood biomarkers to enhance the diagnosis, staging, and prognosis of HCC.

CP is a copper-containing enzyme synthesized primarily in the liver, involved in inflammatory responses and metal metabolism, such as iron and copper[16]. Historically, CP protein has been associated with metabolic disorders like Wilson's disease[17]. For HCC, the role of CP protein levels has been highlighted in several studies. Pousset[18] reported elevated CP protein levels in the blood of experimental HCC in mice. Yang[19] observed increased ceruloplasmin protein levels in the serum of HCC patients. Ferrin[20] suggested that serum CP protein level, in combination with fibrinogen alpha chain (FGA) and paraoxonase 1 (PON1), could be a potential diagnostic marker for HCC in hepatitis C virus-infected individuals.

In contrast, *CP* mRNA has been less frequently investigated. Fifteen years ago, studies by Tseng et al.[21] and Tan et al.[22] found lower *CP* mRNA levels in HCC tissue compared to adjacent non-tumor liver tissue. These findings appear to be at odds with our results, which show elevated *CP* mRNA levels in the blood of HCC patients. This discrepancy might be explained by the hypothesis that HCC induces changes in the surrounding liver tissue,

leading to increased *CP* mRNA production and its subsequent release into the bloodstream. Explaining the mechanisms behind the elevated *CP* mRNA levels in the serum of HCC patients may involve two primary hypotheses. Firstly, HCC patients often exhibit increased expression of the GPC3 gene[23–25]. Consequently, this upregulation leads to the downregulation of the *metallothionein* (*MT*) gene family, which plays a crucial role in heavy metal metabolism[25,26]. The suppression of these genes reduces the HCC cells' ability to bind free copper (Cu2 +), resulting in elevated interstitial copper levels surrounding the tumor[25,26]. This elevation in interstitial copper levels, in turn, stimulates the surrounding non-tumor liver cells to increase *CP* mRNA synthesis, leading to higher *CP* mRNA levels in the blood[27]. Additionally, the reduced expression of hepcidin (HAMP) in HCC tumors leads to the movement of iron from healthy liver cells into the interstitial fluid, decreasing intracellular iron levels[28]. Consequently, this reduction in intracellular iron levels subsequently stimulates increased *CP* mRNA synthesis in the surrounding healthy liver cells, leading to higher *CP* mRNA levels in the blood[29,30].

Conclusions

This study established a novel semi-nested RT-PCR assay for quantifying circulating *CP* mRNA in peripheral blood, highlighting its potential as a non-invasive biomarker for HCC detection. The assay demonstrated the ability to detect HCC in a significant proportion of patients with AFP levels below 20 ng/mL, underscoring its complementary role to AFP. While offering preliminary evidence of its diagnostic value, particularly in early detection and monitoring, these findings remain exploratory due to the retrospective design. Further validation with larger, prospective cohorts is necessary to confirm its clinical applicability and integrate it into routine practice.

Data availability

The datasets generated and/or analysed during the current study, including individual patient data on circulating *CP* mRNA levels for both hepatocellular carcinoma patients and control groups, are available from the corresponding author upon reasonable request. The aggregated and analyzed data have been presented within the manuscript. Requests for access to the individual patient data should be directed to Dr. Tho Huu Ho at hohuutho@vmmu.edu.vn.

Received: 10 June 2024; Accepted: 18 April 2025
Published online: 26 April 2025

References

1. Sung, H. et al. Global cancer statistics 2020: GLOBOCAN estimates of incidence and mortality worldwide for 36 cancers in 185 countries. *CA Cancer J. Clin.* **71**(3), 209–249 (2021).
2. Kim, E. & Viatour, P. Hepatocellular carcinoma: old friends and new tricks. *Exp. Mol. Med.* **52**(12), 1898–1907 (2020).
3. Kim, T. H. et al. Comparison of international guidelines for noninvasive diagnosis of hepatocellular carcinoma: 2018 update. *Clin. Mol. Hepatol.* **25**(3), 245–263 (2019).
4. Neuberger, J. et al. Guidelines on the use of liver biopsy in clinical practice from the British Society of Gastroenterology, the Royal College of Radiologists and the Royal College of Pathology. *Gut* **69**(8), 1382–1403 (2020).
5. Inoue, T. & Tanaka, Y. Novel biomarkers for the management of chronic hepatitis B. *Clin. Mol. Hepatol.* **26**(3), 261–279 (2020).
6. Marrugo-Ramírez, J., Mir, M. & Samitier, J. Blood-based cancer biomarkers in liquid biopsy: A promising non-invasive alternative to tissue biopsy. *Int. J. Mol. Sci.* **19**(10), 2877 (2018).
7. Larson, M. H. et al. A comprehensive characterization of the cell-free transcriptome reveals tissue- and subtype-specific biomarkers for cancer detection. *Nat. Commun.* **12**(1), 2357 (2021).
8. Hassan, S. et al. Diagnostic and therapeutic potential of circulating-free DNA and cell-free RNA in cancer management. *Biomedicines* **10**(8), 2047 (2022).
9. Roskams-Hieter, B. et al. Plasma cell-free RNA profiling distinguishes cancers from pre-malignant conditions in solid and hematologic malignancies. *NPJ Precis. Oncol.* **6**(1), 28 (2022).
10. Pös, O. et al. Circulating cell-free nucleic acids: Characteristics and applications. *Eur. J. Hum. Genet.* **26**(7), 937–945 (2018).
11. Marrero, J. A. et al. Diagnosis, staging, and management of hepatocellular carcinoma: 2018 Practice guidance by the american association for the study of liver diseases. *Hepatology* **68**(2), 723–750 (2018).
12. Kim, H. J. et al. Selective enrichment of plasma cell-free messenger RNA in cancer-associated extracellular vesicles. *Commun. Biol.* **6**(1), 885 (2023).
13. Kudo, M. et al. Management of hepatocellular carcinoma in Japan: JSH consensus statements and recommendations 2021 update. *Liver Cancer* **10**(3), 181–223 (2021).
14. Pan, Y., Chen, H. & Yu, J. Biomarkers in hepatocellular carcinoma: Current status and future perspectives. *Biomedicines* **8**(12), 576 (2020).
15. Chen, Y. et al. Comparison of diagnostic performance of AFP, DCP and two diagnostic models in hepatocellular carcinoma: A retrospective study. *Ann. Hepatol.* **28**(4), 101099 (2023).
16. Musci, G., Polticelli, F. & Bonaccorsi di Patti, M. C. Ceruloplasmin-ferroportin system of iron traffic in vertebrates. *World J. Biol. Chem.* **5**(2), 204–215 (2014).
17. Hellman, N. E. & Gitlin, J. D. Ceruloplasmin metabolism and function. *Annu. Rev. Nutr.* **22**, 439–458 (2002).
18. Pousset, D. et al. High levels of ceruloplasmin in the serum of transgenic mice developing hepatocellular carcinoma. *Eur. J. Biochem.* **268**(5), 1491–1499 (2001).
19. Yang, M. H. et al. Identification of human hepatocellular carcinoma-related proteins by proteomic approaches. *Anal. Bioanal. Chem.* **388**(3), 637–643 (2007).
20. Ferrín, G. et al. Plasma protein biomarkers of hepatocellular carcinoma in HCV-infected alcoholic patients with cirrhosis. *PLoS ONE* **10**(3), e0118527 (2015).
21. Tseng, H. H. et al. Expression of hepcidin and other iron-regulatory genes in human hepatocellular carcinoma and its clinical implications. *J. Cancer Res. Clin. Oncol.* **135**(10), 1413–1420 (2009).
22. Tan, M. G. et al. Modulation of iron-regulatory genes in human hepatocellular carcinoma and its physiological consequences. *Exp. Biol. Med. (Maywood)* **234**(6), 693–702 (2009).
23. Guo, M. et al. Glypican-3: A new target for diagnosis and treatment of hepatocellular carcinoma. *J. Cancer* **11**(8), 2008–2021 (2020).
24. Wu, Y., Liu, H. & Ding, H. GPC-3 in hepatocellular carcinoma: Current perspectives. *J. Hepatocell. Carcinoma* **3**, 63–67 (2016).

25. Hu J., Gao Z. (2014). Data-based core genes screening for Hepatocellular Carcinoma. In *2014 9th IEEE Conference on Industrial Electronics and Applications*: 1102–7.
26. Himoto, T. & Masaki, T. Current trends on the involvement of zinc, copper, and selenium in the process of hepatocarcinogenesis. *Nutrients* **16**(4), 472 (2024).
27. Das, D. et al. Regulation of ceruloplasmin in human hepatic cells by redox active copper: Identification of a novel AP-1 site in the ceruloplasmin gene. *Biochem. J.* **402**(1), 135–141 (2007).
28. Joachim, J. H. & Mehta, K. J. Hepcidin in hepatocellular carcinoma. *Br. J. Cancer* **127**(2), 185–192 (2022).
29. Mukhopadhyay, C. K., Attieh, Z. K. & Fox, P. L. Role of ceruloplasmin in cellular iron uptake. *Science* **279**(5351), 714–717 (1998).
30. Mukhopadhyay, C. K., Mazumder, B. & Fox, P. L. Role of hypoxia-inducible factor-1 in transcriptional activation of ceruloplasmin by iron deficiency. *J. Biol. Chem.* **275**(28), 21048–21054 (2000).

Acknowledgements

We thank Thuy Minh Thi Ngo for valuable discussion; Dung Huu Nguyen, Tu Cam Vu, Kim Ngan Thi Dinh, Quyen Van Pham, Yen Hai Tran, Quyen Thi Nguyen, and Thu Hang Pham for their exceptional technical assistance.

Author contributions

Conceptualization, Minh Ngo, Huy Duong, Jakob Stenman and Tho Ho; Formal analysis, Minh Ngo, Trang Dao, Trang Hoang, Ung Nguyen and Tho Ho; Methodology, Minh Ngo, Trang Dao, Trang Hoang, Ung Nguyen, Jakob Stenman, Huy Duong and Tho Ho; Validation, Minh Ngo, Trang Dao, Trang Hoang, Ung Nguyen and Tho Ho; Writing—original draft, Minh Ngo, Trang Dao and Tho Ho; Writing—review and editing, Minh Ngo, Trang Dao, Ung Nguyen, Jakob Stenman, Huy Duong and Tho Ho. All authors have read and agreed to the published version of the manuscript.

Declarations

Competing interests

The authors declare no competing interests.

Ethics

All procedures performed in studies involving human participants were in accordance with the ethical standards of the institutional research committee of 103 Military Hospital, Vietnam Military Medical University (reference number: 12/2021/CNChT-HĐĐĐ, dated 28/06/2021) and with the 1964 Helsinki declaration and its later amendments or comparable ethical standards. Informed consent was obtained from all individual participants included in the study.

Additional information

Supplementary Information The online version contains supplementary material available at https://doi.org/10.1038/s41598-025-99302-3.

Correspondence and requests for materials should be addressed to T.H.